4-1-2021

Reduced-order fast converging observers for systems with discrete measurements and measurement error

Frédéric Mazenc
Laboratoire des Signaux et Systèmes

Michael Malisoff
Louisiana State University

Zhong Ping Jiang
NYU Tandon School of Engineering

Reduced-Order Fast Converging Observers for Systems with Discrete Measurements and Measurement Error

Frederic Mazenc, Michael Malisoff, Zhong-Ping Jiang

Reduced-Order Fast Converging Observers for Systems with Discrete Measurements and Measurement Error ⋆

Frédéric Mazenc [a] Michael Malisoff [b] Zhong-Ping Jiang [c]

[a] *Inria EPI DISCO, L2S-CNRS-CentraleSupélec, 3 rue Joliot Curie, 91192, Gif-sur-Yvette, France (e-mail: frederic.mazenc@l2s.centralesupelec.fr)*

[b] *Department of Mathematics, Louisiana State University, Baton Rouge, LA 70803-4918, USA (email: malisoff@lsu.edu)*

[c] *Department of Electrical and Computer Engineering, Tandon School of Engineering, New York University, Brooklyn, NY 11201, USA (email: zjiang@nyu.edu)*

Abstract

We provide novel reduced-order observer designs for continuous-time nonlinear systems with measurement error. Our first result applies to systems with continuous output measurements, and provides observers that converge in a fixed finite time that is independent of the initial state when the measurement error is zero. Our second result applies under discrete measurements, and provides observers that converge asymptotically with a rate of convergence that is proportional to the negative of the logarithm of the size of a sampling interval. Our observers satisfy an enhanced input-to-state stability property with respect to the measurement error, in which an overshoot term only depends on a recent history of the measurement error. We illustrate our observers using a model of a single-link robotic manipulator coupled to a DC motor with a nonrigid joint, and in a pendulum example.

Key words: Reduced-order observer, finite time, discrete measurements

1 Introduction

Finite time observers offer considerable promise for an ever-growing range of practical applications, because of their ability to compute exact values of states in a finite time. Several finite time observer designs are available; see for instance the works by Ahmed *et al.* (2019), Engel and Kreisselmeier (2002), Lebastard *et al.* (2006), Lopez-Ramirez *et al.* (2018), Mazenc *et al.* (2015), Menard *et al.* (2010), Raff *et al.* (2005), Sanchez-Torres *et al.* (2012), Sauvage *et al.* (2007), and Zhao and Jiang (2019). The preceding works use delays, dynamic extensions, homogenous functions, and sliding mode. The work by Raff and Allgower (2008) differs significantly from the others, because it is based on a continuous-discrete observer that does not incorporate delays and therefore may be easier to implement than observers that incorporate delays. Moreover, since Raff and Allgower (2008) does not use homogeneity properties, it can enjoy better robustness compared with other observer methods. On the other hand, while the observers in Raff and Allgower (2008) are of continuous-discrete type, its methods only apply to linear systems and they require values of a continuous output, and so is not suitable when only discrete measurements are available.

Therefore, this paper builds on Raff and Allgower (2008) in the context of a family of nonlinear continuous-time systems. In addition to generalizing Raff and Allgower (2008) to nonlinear systems, this paper provides these other contributions. First, when the measurements are continuous, we provide a reduced-order version of the observer from Raff and Allgower (2008) (insofar that our observer has a lower dimension than the one in Raff and Allgower (2008)) that has the additional advantage of ensuring finite time convergence when the measurement error is zero, where the convergence time can be selected by the user. This fixed time convergence property means that the convergence time is independent of the initial state. The fixed time is twice the sample rate, and the sample rate must be chosen to satisfy an invertibility condition that involves the coefficient matrices in the original system; see Section 2 below. This differs from semi-global works such as Zhao and Jiang (2019) whose finite convergence time depends on the initial state.

When measurement error is present, our result for the continuous measurements case provides an enhanced input-to-state stability (or ISS) property, where the sup norm of the

⋆ Supported by US National Science Foundation Grants 1903781 (Jiang) and 1711299 (Malisoff). The authors thank Mr. Leilei Cui for assisting with the simulations in Section 5. Special cases of this work will appear in the conference paper Mazenc *et al.* (2020); see Section 1 for a comparison between this work and the conference version.

uncertain measurement error in the upper bound on the observation error is only over a recent history of the uncertainty. This differs from standard ISS, whose supremum is over the entire past history of the uncertainty starting from the initial time. We require a global Lipschitzness condition to obtain our enhanced ISS condition. However, our method for cases with continuous time observations applies without global Lipschitzness conditions when the measurement error is zero. This allows Hölder continuous dynamics that are not globally Lipschitz. On the other hand, a limitation of this first result is that it does not apply when the measurements are only available at discrete times.

Therefore, we also provide a second observer design for a family of nonlinear systems that satisfies a global Lipschitzness condition whose measurements are only available at discrete times, which is based on combining our first result with a key approach of Karafyllis and Kravaris (2009) that was also used in Karafyllis and Jiang (2013). The price to pay for allowing discrete measurements is that this second observer does not satisfy a finite time convergence property. However, it is also of reduced-order and is helpful in terms of speed of convergence when the size of the sampling intervals is small, because its convergence speed is proportional to the negative of the logarithm of an upper bound on sampling interval lengths. This improves on asymptotic observers (such as those of Besançon (2007)) that did not provide this type of convergence rate guarantee. Our work also contrasts with the interval observer approach in Mazenc *et al.* (2015), because we do not have integrals in our exact state construction in the unperturbed case with continuous output measurements, and because we can ensure arbitrarily fast convergence when the output measurements contain sampling and uncertainty.

Our convergence proof for our second observer uses a recent trajectory based approach, which was developed in Ahmed *et al.* (2018) and Mazenc *et al.* (2017). As in the case of continuous measurements, we show how this second observer design provides an enhanced ISS property with respect to measurement noise, where the upper bound on the observation error only depends on a recent history of the measurement error. We illustrate our second observer design using a pendulum model that was studied in Dinh *et al.* (2015) in the full order observer case, and we include measurement error in this illustration that was also beyond the scope of Dinh *et al.* (2015). This paper improves on our conference version Mazenc *et al.* (2020) which did not allow measurement error and did not include the application to robotic manipulators, and in addition, this paper provides less conservative conditions on the sample times in our second theorem as compared with Mazenc *et al.* (2020); see Remark 4 below.

This paper is arranged as follows. In Section 2, we present the systems under study. In Section 3, we provide our observer design for continuous measurements, and Section 4 provides results for discrete measurements. Our illustrative examples for the robotic manipulator and the pendulum are in Section 5. Concluding remarks are in Section 6.

Notation. We use standard notation, which we simplify when no confusion would arise. The dimensions of our Euclidean spaces are arbitrary, unless we indicate otherwise. The standard Euclidean 2-norm, and its induced matrix norm, are denoted by $|\cdot|$, $|\cdot|_\infty$ is the usual $\mathcal{L}_\infty$ sup norm, $|\cdot|_S$ denotes the essential supremum over any set S, $\mathbb{N} = \{1, 2, \ldots\}$, and $\mathbb{Z}_{\geq 0} = \{0\} \cup \mathbb{N}$. For any piecewise continuous locally bounded function $\phi : [0, +\infty) \to \mathbb{R}^m$ having a left limit at a point c, we use $\phi(c^-)$ to denote the left limit $\phi(c^-) = \lim_{t\to c^-} \phi(t)$. Also, $0_{m\times n}$ (resp., I_n) denotes the $m \times n$ matrix whose entries are all 0 (resp., the $n \times n$ identity matrix). We also use $\lfloor\ \rfloor$ to denote the floor function, so $\lfloor x \rfloor = \max\{p \in \mathbb{Z}_{\geq 0} : p \leq x\}$ for all $x \geq 0$.

2 Studied system

We consider the system

$$\dot{x}(t) = Ax(t) + f(r(t), u(t)) \tag{1}$$

with $x(t)$ valued in $\mathbb{R}^n$, the input $u(t)$ valued in $\mathbb{R}^q$, and $A \in \mathbb{R}^{n\times n}$, where f is a locally Lipschitz nonlinear function that satisfies $f(0_{p\times 1}, 0_{q\times 1}) = 0_{n\times 1}$ and

$$r(t) = Cx(t) \tag{2}$$

with $r(t)$ valued in $\mathbb{R}^p$ and $C \in \mathbb{R}^{p\times n}$, and with $p < n$. Throughout the paper, we assume:

Assumption 1 *The rank of C is full. The pair (A, C) is observable.* □

Under Assumption 1, it is well known that (1) can be transformed into a system of the form

$$\begin{cases} \dot{r}(t) = F_{11}r(t) + F_{12}x_r(t) + f_1(r(t), u(t)) \\ \dot{x}_r(t) = F_{21}r(t) + F_{22}x_r(t) + f_2(r(t), u(t)) \end{cases} \tag{3}$$

through a linear change of coordinates of the form

$$\begin{bmatrix} x_r(t) \\ r(t) \end{bmatrix} = \mho x(t) \tag{4}$$

with an invertible matrix $\mho$, with

$$\mho A \mho^{-1} = \begin{bmatrix} F_{22} & F_{21} \\ F_{12} & F_{11} \end{bmatrix}, \ \mho = \begin{bmatrix} V \\ C \end{bmatrix}, \qquad f_1 = Cf,\ f_2 = Vf,\ V \in \mathbb{R}^{(n-p)\times n}, \tag{5}$$

$F_{11} \in \mathbb{R}^{p\times p}$, $F_{12} \in \mathbb{R}^{p\times(n-p)}$, $F_{21} \in \mathbb{R}^{(n-p)\times p}$ and $F_{22} \in \mathbb{R}^{(n-p)\times(n-p)}$, where (F_{22}, F_{12}) is an observable pair; see (Luenberger, 1979, pp.304-306). As shown in Mazenc *et al.* (2015), we can then find a matrix $L \in \mathbb{R}^{(n-p)\times p}$ and a constant $\nu > 0$ (that can be taken to be arbitrarily large) so that with the choice

$$H = F_{22} + LF_{12} \in \mathbb{R}^{(n-p)\times(n-p)}, \tag{6}$$

the matrix

$$E = e^{-F_{22}\nu} - e^{-H\nu} \tag{7}$$

is invertible. Therefore ν depends on L, F_{12}, and F_{22} and so depends on the model parameters. As noted in Mazenc *et al.* (2015), such a ν can be found by first choosing L such that H is Hurwitz. Next, we introduce the sequence

$$t_i = i\nu \text{ for all } i \in \mathbb{Z}_{\geq 0}, \tag{8}$$

the matrices

$$\begin{aligned} G &= F_{21} - F_{22}L + LF_{11} - LF_{12}L \\ &= F_{21} + LF_{11} - HL \in \mathbb{R}^{(n-p)\times p}, \\ R_1 &= E^{-1}e^{-\nu F_{22}} \in \mathbb{R}^{(n-p)\times(n-p)} \text{ and} \\ R_2 &= -E^{-1}e^{-\nu H} \in \mathbb{R}^{(n-p)\times(n-p)} \end{aligned} \tag{9}$$

and the $\mathbb{R}^{n-p}$-valued function

$$f_3 = f_2 + Lf_1. \tag{10}$$

3 Observer when the output is continuous

3.1 Observer

We will first consider (1) and the case where the output is

$$y(t) = r(t) + \epsilon(t), \tag{11}$$

where the piecewise continuous locally bounded function $\epsilon : [0, \infty) \to \mathbb{R}^p$ represents measurement error, and then (in Section 4) we study discrete outputs. In order to ensure our enhanced ISS property with respect to the measurement error ϵ in (11), we also make the following global Lipschitzness assumption, but this assumption is not required in our first theorem when ϵ is the zero function:

Assumption 2 *There is a constant $f_\dagger > 0$ such that*

$$|f(m_1, u) - f(m_2, u)| \leq f_\dagger|m_1 - m_2| \tag{12}$$

for all $m_1 \in \mathbb{R}^p, m_2 \in \mathbb{R}^p$ and $u \in \mathbb{R}^q$. □

It follows from Assumption 2 that there are constants $f_{\dagger,1} > 0$ and $f_{\dagger,2} > 0$ such that

$$|f_1(m_1, u) - f_1(m_2, u)| \leq f_{\dagger,1}|m_1 - m_2| \tag{13}$$

$$|f_2(m_1, u) - f_2(m_2, u)| \leq f_{\dagger,2}|m_1 - m_2| \tag{14}$$

hold for all $m_1 \in \mathbb{R}^p, m_2 \in \mathbb{R}^p$ and $u \in \mathbb{R}^q$, where the positivity of $f_{\dagger,1}$ is needed to ensure positivity of an ln argument below when $F_{21} = 0$; see (40) and (43). Using our fixed constant $\nu > 0$ from above, we also use

$$\overline{E} = |E^{-1}| \tag{15}$$

and

$$f_{\dagger,3} = f_{\dagger,2} + |L|f_{\dagger,1}. \tag{16}$$

With our output (11), we consider the dynamic extension

$$\begin{cases} \dot{z}_1(t) &= F_{21}y(t) + F_{22}z_1(t) + f_2(y(t), u(t)) \\ & \quad \text{if } t \in [t_k, t_{k+1}) \\ \dot{z}_2(t) &= Hz_2(t) + Gy(t) + f_3(y(t), u(t)) \\ & \quad \text{if } t \in [t_k, t_{k+1}) \\ z_1(t_{k+1}) &= R_1 z_1(t_{k+1}^-) + R_2 z_2(t_{k+1}^-) \\ & \quad -R_2Ly(t_{k+1}) - E^{-1}Ly(t_k) \\ z_2(t_{k+1}) &= R_1 z_1(t_{k+1}^-) + R_2 z_2(t_{k+1}^-) \\ & \quad -R_2Ly(t_{k+1}) - E^{-1}Ly(t_k) \end{cases} \tag{17}$$

for all integers $k \geq 0$, with $z_1(0) = z_2(0) = 0$, but our theorems remain true if we fix any other initial states for the z_i's at time 0. Although the output measurements are available for all times $t \geq 0$, our choice of (17) is motivated by the need to update the z_1 and z_2 measurements to produce a global convergence result.

The solutions of (17) are defined as follows. Starting the zero initial states, we use the systems of differential equations in (17) to solve for $z_1(t)$ and $z_2(t)$ on the interval $[t_0, t_1) = [0, \nu)$. Then, at time t_1, we reset the states z_1 and z_2 to their new values, as defined in the last two equations of (17). Then, starting from these values of $z_1(t_1)$ and $z_2(t_1)$, we use the differential equations in (17) to solve for $z_1(t)$ and $z_2(t)$ on the interval $[t_1, t_2) = [\nu, 2\nu)$, and then we repeat this process inductively.

In terms of the constants

$$\begin{aligned} J_1 &= |F_{21}| + f_{\dagger,2} \text{ and} \\ J_2 &= |E^{-1}e^{-\nu H}L| + |E^{-1}L| + \int_{-\nu}^{0} |E^{-1}e^{\ell F_{22}}F_{21}|\mathrm{d}\ell \\ &\quad + \int_{-\nu}^{0} |E^{-1}e^{\ell H}G|\mathrm{d}\ell + f_{\dagger,2}\int_{-\nu}^{0} |E^{-1}e^{\ell F_{22}}|\mathrm{d}\ell \\ &\quad + f_{\dagger,3}\int_{-\nu}^{0} |E^{-1}e^{\ell H}|\mathrm{d}\ell \end{aligned} \tag{18}$$

and our sequence $t_i = i\nu$ from (8), we prove:

Theorem 1 *If the system (1) satisfies Assumptions 1-2, then for each initial state $x(0) \in \mathbb{R}^n$, the solution of (3) and (17) is such that*

$$|z_1(t) - x_r(t)| \leq e^{|F_{22}|(t-\nu\lfloor t/\nu \rfloor)}(\nu J_1 + J_2)|\epsilon|_{[t-2\nu,t]} \tag{19}$$

holds for all $t \geq t_2$. □

Remark 1 Notice that L affects J_2 and therefore affects the size of the overshoot and the impact of the uncertainty ϵ on the performance of our observer. Our ability to allow arbitrarily large ν values is analogous to the fact that predictive delay compensating controllers or predictive observers can compensate for arbitrarily long delays, because sampling can be viewed as a time-varying sawtooth shaped delay. Also, the norm of ϵ in (19) is defined because of our condition $t \geq t_2 = 2\nu$. An important distinction between our observer (17) and the one in Raff and Allgower (2008) is that the dimension of our $z = (z_1, z_2)$-subsystem in (17) is $2(n - p)$, while the dimension of the corresponding system in Raff and Allgower (2008) is $2n$.

Compared with the significant work by Menard *et al.* (2017), potential advantages of Theorem 1 are that (i) the result is global (for all initial states of the original system), which contrasts with the local results of Menard *et al.* (2017) for cases with nonzero uncertainties and (ii) the fact that the supremum of ϵ in our bound on $|z_1(t) - x_r(t)|$ from Theorem 1 is only over a recent history of ϵ, instead of a supremum of ϵ from the initial time to the current time. □

Remark 2 As noted above, in the special case where the measurement error ϵ is the zero function, Theorem 1 remains true if we omit its Assumption 2. In that special case, the function $r(t) = Cx(t)$ is available for measurement, so since $z_1(t)$ is also known for all $t \geq t_0$, it follows from Theorem 1 that $x(t)$ is known for all $t \geq t_2$ because (4) implies

$$x(t) = \mho^{-1} \begin{pmatrix} z_1(t) \\ y(t) \end{pmatrix} \tag{20}$$

for all $t \geq t_2$. □

3.2 Proof of Theorem 1

We use the variable

$$\xi(t) = x_r(t) + Lr(t), \tag{21}$$

where $r(t) = Cx(t)$ as before. Then (3) gives

$$\begin{aligned} \dot{\xi}(t) &= (F_{21} + LF_{11})r(t) + (F_{22} + LF_{12})x_r(t) \\ &\quad + f_3(r(t), u(t)) \\ &= (F_{21} + LF_{11})r(t) + (F_{22} \\ &\quad + LF_{12})(\xi(t) - Lr(t)) + f_3(r(t), u(t)). \end{aligned} \tag{22}$$

Hence, our choices of G and H in (6) and (9) give

$$\begin{cases} \dot{x}_r(t) = F_{21}r(t) + F_{22}x_r(t) + f_2(r(t), u(t)) \\ \dot{\xi}(t) = H\xi(t) + Gr(t) + f_3(r(t), u(t)). \end{cases} \tag{23}$$

Given any $k \in \mathbb{Z}_{\geq 0}$, we apply the method of variation of parameters to the differential equations in (17) and (23) on $[t_k, t_{k+1})$ to obtain

$$\begin{aligned} & e^{-\nu F_{22}} x_r(t_{k+1}) = x_r(t_k) \\ & + \int_{t_k}^{t_{k+1}} e^{(t_{k+1}-\ell-\nu)F_{22}} \left[F_{21}r(\ell) + f_2(r(\ell), u(\ell))\right] \mathrm{d}\ell \\ & \text{and } \; e^{-\nu H}\xi(t_{k+1}) = \xi(t_k) \\ & + \int_{t_k}^{t_{k+1}} e^{(t_{k+1}-\ell-\nu)H} \left[Gr(\ell) + f_3(r(\ell), u(\ell))\right] \mathrm{d}\ell \\ & \text{and } \; e^{-\nu F_{22}} z_1(t_{k+1}^-) = z_1(t_k) \\ & + \int_{t_k}^{t_{k+1}} e^{(t_{k+1}-\ell-\nu)F_{22}} \left[F_{21}y(\ell) + f_2(y(\ell), u(\ell))\right] \mathrm{d}\ell \\ & \text{and } \; e^{-\nu H} z_2(t_{k+1}^-) = z_2(t_k) \\ & + \int_{t_k}^{t_{k+1}} e^{(t_{k+1}-\ell-\nu)H} \left[Gy(\ell) + f_3(y(\ell), u(\ell))\right] \mathrm{d}\ell. \end{aligned} \tag{24}$$

In terms of the function

$$\begin{aligned} & \mathcal{G}(t, s, \omega) = \int_s^t \left[e^{(s-\ell)F_{22}} F_{21} - e^{(s-\ell)H} G\right] \omega(\ell) \mathrm{d}\ell \\ & + \int_s^t \left[e^{(s-\ell)F_{22}} f_2(\omega(\ell), u(\ell)) - e^{(s-\ell)H} f_3(\omega(\ell), u(\ell))\right] \mathrm{d}\ell, \end{aligned} \tag{25}$$

it follows from subtracting the second equation of (24) from the first equation of (24) and our choice (7) of E that

$$\begin{aligned} & Ex_r(t_{k+1}) - e^{-\nu H} Ly(t_{k+1}) + Ly(t_k) \\ & = \mathcal{G}(t_{k+1}, t_k, r) + \mathcal{L}_k(\epsilon), \end{aligned} \tag{26}$$

where

$$\mathcal{L}_k(\epsilon) = -e^{\nu H} L\epsilon(t_{k+1}) + L\epsilon(t_k),$$

and where we used the fact that $\xi = x_r + Lr = x_r + L(y - \epsilon)$. Since $z_1(t_k) = z_2(t_k)$ for all $k \geq 1$, it follows from the last two equations of (24) that

$$e^{-\nu F_{22}} z_1(t_{k+1}^-) - e^{-\nu H} z_2(t_{k+1}^-) = \mathcal{G}(t_{k+1}, t_k, y) \tag{27}$$

for all $k \geq 1$. In terms of the function

$$\Delta\mathcal{G}(t, s, \omega, \Omega) = \mathcal{G}(t, s, \omega) - \mathcal{G}(t, s, \Omega), \tag{28}$$

it follows that if we combine (26) and (27), then we obtain

$$\begin{aligned} & Ex_r(t_{k+1}) - e^{-\nu H} Ly(t_{k+1}) + Ly(t_k) \\ & = e^{-\nu F_{22}} z_1(t_{k+1}^-) - e^{-\nu H} z_2(t_{k+1}^-) \\ & + \Delta\mathcal{G}(t_{k+1}, t_k, r, y) + \mathcal{L}_k(\epsilon). \end{aligned} \tag{29}$$

Since E is invertible, this gives

$$\begin{aligned} x_r(t_{k+1}) &= E^{-1} e^{-\nu H} Ly(t_{k+1}) - E^{-1} Ly(t_k) \\ &\quad + E^{-1} \mathcal{L}_k(\epsilon) + R_1 z_1(t_{k+1}^-) \\ &\quad + R_2 z_2(t_{k+1}^-) + E^{-1} \Delta\mathcal{G}(t_{k+1}, t_k, r, y) \\ &= z_1(t_{k+1}) + E^{-1} \mathcal{L}_k(\epsilon) \\ &\quad + E^{-1} \Delta\mathcal{G}(t_{k+1}, t_k, r, y), \end{aligned} \tag{30}$$

where the last equality in (30) follows from the formula for $z_1(t_{k+1})$ in (17) and our choice of R_2 in (9). Recalling that $y - r = \epsilon$, and that f_2 and f_3 admit the global Lipschitz constants $f_{\dagger,2}$ and $f_{\dagger,3}$ respectively in their first variables uniformly in their second variable, it follows from our choices (18) of J_1 and J_2 that

$$|z_1(t_{k+1}) - x_r(t_{k+1})| \leq J_2 |\epsilon|_{[t_k, t_{k+1}]} \tag{31}$$

for all $k \in \mathbb{N}$, and

$$|\dot{z}_1(t) - \dot{x}_r(t)| \leq J_1 |\epsilon(t)| + |F_{22}||x_r(t) - z_1(t)| \tag{32}$$

for all $t \in [t_k, t_{k+1})$ and $k \in \mathbb{Z}_0$. Using (31)-(32), we can now apply the Fundamental Theorem of Calculus to $z_1 - x_r$ on each interval $[t_{k+1}, t_{k+2})$ for $k \in \mathbb{N}$ to get

$$\begin{aligned} |z_1(t) - x_r(t)| &\leq \nu J_1 |\epsilon|_{[t_{k+1}, t]} + J_2 |\epsilon|_{[t_k, t_{k+1}]} \\ &\quad + \int_{t_{k+1}}^t |F_{22}||x_r(\ell) - z_1(\ell)| \mathrm{d}\ell, \end{aligned} \tag{33}$$

and then we can apply Gronwall's inequality to $|z_1 - x_r|$ on each of these intervals to obtain

$$\begin{aligned} & |z_1(t) - x_r(t)| \leq \\ & \left(J_2 |\epsilon|_{[t_k, t_{k+1}]} + J_1 \nu |\epsilon|_{[t_{k+1}, t]}\right) e^{|F_{22}|(t - t_{k+1})} \end{aligned} \tag{34}$$

for all $t \in [t_{k+1}, t_{k+2})$ and all $k \in \mathbb{N}$. Hence, the conclusion of Theorem 1 follows from our choice of ν, because $[t_k, t_{k+1}] \subseteq [t - 2\nu, t]$, $[t_{k+1}, t] \subseteq [t - \nu, t]$, and $t_{k+1} = \nu \lfloor t/\nu \rfloor$ all hold for all $t \in [t_{k+1} t_{k+2})$ and $k \in \mathbb{N}$, by our choices of the sample times $t_i = i\nu$ for all i.

4 Observer when the output is discrete

We continue using the notation from Sections 2 and 3. The theorem in this section owes a great deal to the pioneering work by Karafyllis and Kravaris (2009), because we use a dynamic extension from Karafyllis and Kravaris (2009). However, this section allows arbitrarily large convergence rates for our reduced-order observer as well as the enhanced ISS property that we obtained in the continuous measurements case from Theorem 1. These notable features were beyond the scope of Karafyllis and Kravaris (2009).

Given a constant $\mu > 0$, we use the sequence

$$s_i = i\mu \tag{35}$$

for all $i \in \mathbb{Z}_{\geq 0}$, and the system

$$\begin{cases} \dot{x}(t) = Ax(t) + f(r(t), u(t)) \\ y(t) = Cx(s_j) + \epsilon(s_j) \text{ if } t \in [s_j, s_{j+1}) \\ r(t) = Cx(t) \end{cases} \tag{36}$$

where the unknown piecewise continuous locally bounded function ϵ in the measured output y again represents measurement error, and we add:

Assumption 3 *There is a $g \in \mathbb{N}$ such that $\nu = g\mu$, where ν satisfies the requirements from Section 2.* □

Our added Assumption 3 is not restrictive, because ν and g can be arbitrarily large.

4.1 Observer

We will use the following as our observer:

$$\begin{cases} \dot{z}_1(t) = F_{21}w(t)+F_{22}z_1(t)+f_2(w(t), u(t)) \\ \quad \text{if } t \in [s_{gk}, s_{g(k+1)}) \\ \dot{z}_2(t) = Hz_2(t) + Gw(t) + f_3(w(t), u(t)) \\ \quad \text{if } t \in [s_{gk}, s_{g(k+1)}) \\ z_1(s_{g(k+1)}) = R_1 z_1(s^-_{g(k+1)}) + R_2 z_2(s^-_{g(k+1)}) \\ \quad -R_2 Ly(s_{g(k+1)}) - E^{-1}Ly(s_{gk}) \\ z_2(s_{g(k+1)}) = R_1 z_1(s^-_{g(k+1)}) + R_2 z_2(s^-_{g(k+1)}) \\ \quad -R_2 Ly(s_{g(k+1)}) - E^{-1}Ly(s_{gk}) \\ \dot{w}(t) = F_{11}w(t)+F_{12}z_1(t)+f_1(w(t), u(t)) \\ \quad \text{if } t \in [s_k, s_{k+1}) \\ w(s_k) = y(s_k) \end{cases} \tag{37}$$

for all $k \in \mathbb{Z}_{\geq 0}$, with $z_1(0) = z_2(0)$. The solutions of (37) are defined using the same inductive procedure that we used to define the solutions of (17). We also use

$$\mathcal{I}^s_+(M) = \int_0^s |e^{\ell M}| \mathrm{d}\ell, \;\; \mathcal{I}^s_-(M) = \int_{-s}^0 |e^{\ell M}| \mathrm{d}\ell, \\ \text{and } \mathcal{F}_s(M) = \sup\{|e^{\ell M}| : 0 \leq \ell \leq s\} \tag{38}$$

for square matrices M and constants $s > 0$, and the constants

$$\begin{aligned} \beta(\nu) = {} & \mathcal{I}^\nu_+(F_{22})(|F_{21}| + f_{\dagger,2}) \\ & + \bar{E}\mathcal{F}_\nu(F_{22})\mathcal{I}^\nu_-(H)\big(|G| + f_{\dagger,3}\big) \\ & + \bar{E}\mathcal{F}_\nu(F_{22})\mathcal{I}^\nu_-(F_{22})\big(|F_{21}| + f_{\dagger,2}\big) \end{aligned} \tag{39}$$

and

$$\gamma(\mu) = \mathcal{I}^\mu_+(F_{11})(\beta(\nu) + 1) \max\{f_{\dagger,1}, |F_{21}|\}. \tag{40}$$

We also fix a constant $\overline{\mu} > 0$ such that

$$\gamma(\mu) \in (0, 1) \text{ for all } \mu \in (0, \overline{\mu}). \tag{41}$$

Since $\nu > 0$ in (40) is a fixed constant that satisfies the requirements from Section 2 (i.e., the invertibility of $E = e^{-F_{22}\nu} - e^{-H\nu}$), it follows that satisfying the requirement $\mu \in (0, \bar{\mu})$ is equivalent to choosing $g \in \mathbb{N}$ in Assumption 3 such that $g = \nu/\mu > \nu/\bar{\mu}$. Using the constant

$$\mathcal{M}_* = \frac{\mathcal{F}_\nu(F_{22})\big(|R_2 L| + |E^{-1}L|\big) + \mathcal{F}_\mu(F_{11})\big(\beta(\nu)+1\big)}{1-\gamma(\mu)}, \tag{42}$$

our main theorem of this section is:

Theorem 2 *Let (36) satisfy Assumptions 1-3 with a constant $\mu \in (0, \overline{\mu})$, where A, C, L, and ν satisfy the observability and invertibility conditions from Section 2. Then for all initial states $x(0) \in \mathbb{R}^n$ and $w(0) \in \mathbb{R}^p$, the solution of of (3) and (37) is defined over $[0, +\infty)$ and satisfies*

$$\begin{aligned} |x_r(t) - z_1(t)| \leq {} & e^{\frac{\ln(\gamma(\mu))}{\mu+2\nu+m}(t-m)} \big(|x_r - z_1|_{[m-(\mu+2\nu),m]} \\ & + |w - r|_{[m-(2\nu+\mu),m]}\big) \\ & + \mathcal{M}_* |\epsilon|_{[t-(2\nu+\mu),t]} \end{aligned} \tag{43}$$

for all $t \geq m$ and all $m \geq 4\nu$. □

Remark 3 One notable feature of (43) is that it provides a rate convergence that is proportional to $-\ln(\gamma(\mu))$. Hence, smaller values of $\mu > 0$ increase the rate of convergence, but smaller μ's require more frequent sampling in the w variable in (37). It is also notable that Theorem 2 provides a $2n - p$ dimensional observer, and so is a reduced-order observer. As in the continuous measurements case from Theorem 1, Theorem 2 provides a global robustness result with respect to measurement uncertainty, in which the overshoot term on the right side of the observation error estimate only depends on a recent history of the measurement error ϵ. Another advantage is that it allows arbitrarily fast convergence under sampled outputs, because its convergence rate $-\ln(\gamma(\mu))$ converges to $+\infty$ as the sample rate μ converges to zero. □

Remark 4 In the special case where ϵ is the zero function, Theorem 2 is less conservative than the corresponding sampled result in Mazenc *et al.* (2020). This is because here, we use $\mathcal{I}^\nu_\pm(M)$ and $\mathcal{I}^\mu_+(F_{11})$ in our β and γ formulas for suitable matrices M, while the corresponding β and γ formulas in Mazenc *et al.* (2020) used the conservative upper bounds $e^{\nu|M|}$ for the integrands in the preceding integrals. This provides less restrictive conditions on μ than Mazenc *et al.* (2020). □

4.2 Proof of Theorem 2

By Assumption 2, the maximal solutions of (3) and (37) are defined over $[0, +\infty)$, since the finite time escape phenomenon does not occur. Our proof has four parts.

Outline of proof. To make the proof easy to follow, we first explain the strategy of the proof. The main strategy is the derive two continuous-discrete dynamics for the error variables $\tilde{w}(t) = w(t) - r(t)$ and $\tilde{x}_r(t) = x_r(t) - z_1(t)$, where the right sides of the systems are expressed in terms of $\tilde{w}$, $\tilde{x}_r$, and the differences $\Delta_i(\ell) = f_i(r(\ell), u(\ell)) - f_i(w(\ell), u(\ell))$ for $i = 1, 2, 3$, and where the states $\tilde{w}$ and $\tilde{x}_r$ are reset at the sample times t_i and s_i respectively. This makes it possible to find upper bounds for $|\tilde{x}_r(t)|$ and $|\tilde{w}(t)|$ that are expressed in terms of $\tilde{x}_r$, $\tilde{w}$, and ϵ, and then we can use the bound on $|\tilde{w}(t)|$ to bound the right side of the $|\tilde{x}_r(t)|$ bound to obtain the final estimate of the theorem.

However, to derive the dynamics for $\tilde{w}$ and $\tilde{x}_r$, we first need to derive a formula for $x_r(t_{k+1})$ in terms of $z_1(t_{k+1})$, ϵ, the Δ_i's, and $w-r$. Therefore, the first step of the proof derives the required formula for $x_r(t_{k+1})$, the second step derives the dynamics for $\tilde{w}$ and the required upper bound for $|\tilde{w}(t)|$, the third step computes the dynamics for $\tilde{x}_r$ and the required upper bound for $|\tilde{x}_r(t)|$, and then the final fourth step combines the bounds $|\tilde{w}(t)|$ and $|\tilde{x}_r(t)|$ to obtain the conclusion of the theorem.

First part of the proof: an expression for $x_r(t_{k+1})$. We first express the sample time values $x_r(t_{k+1})$ in terms of ϵ and the other state and observer values. To this end, set

$$t_k = s_{gk} \tag{44}$$

for all $k \in \mathbb{Z}_{\geq 0}$. Then Assumption 3 gives $t_k = gk\mu = k\nu$ for all $k \in \mathbb{Z}_{\geq 0}$. Hence, this sequence is analogous to the sequence t_k from Section 2. We use the variable

$$\xi(t) = x_r(t) + Lr(t). \tag{45}$$

Then the calculations that led to (23) and our choice $f_3 = f_2 + Lf_1$ again give

$$\dot{\xi}(t) = H\xi(t) + Gr(t) + f_3(r(t), u(t)). \tag{46}$$

Then, for any $k \in \mathbb{Z}_{\geq 0}$, we can apply variation of parameters to (3), (37), and (46) on the interval $[t_k, t_{k+1})$ to obtain (24) except with y in the last two equations of (24) replaced by w. By subtracting the second equation of (24) from the first equation of (24), it follows from (3) and the fact that

$$z_1(t_j) - z_2(t_j) = 0 \tag{47}$$

for all $j \geq 1$ that

$$\begin{aligned} &e^{-\nu F_{22}} x_r(t_{k+1}) - e^{-\nu H}\xi(t_{k+1}) + Lr(t_k) \\ &= \int_{t_k}^{t_{k+1}} e^{(t_k-\ell)F_{22}} F_{21} w(\ell)\mathrm{d}\ell - \int_{t_k}^{t_{k+1}} e^{(t_k-\ell)H} G w(\ell)\mathrm{d}\ell \\ &+ \int_{t_k}^{t_{k+1}} \left[e^{(t_k-\ell)H}G - e^{(t_k-\ell)F_{22}}F_{21}\right](w(\ell)-r(\ell))\mathrm{d}\ell \\ &+ \int_{t_k}^{t_{k+1}} e^{(t_k-\ell)F_{22}} f_2(r(\ell), u(\ell))\mathrm{d}\ell \\ &- \int_{t_k}^{t_{k+1}} e^{(t_k-\ell)H} f_3(r(\ell), u(\ell))\mathrm{d}\ell \end{aligned} \tag{48}$$

and

$$\begin{aligned} &e^{-\nu F_{22}} z_1(t_{k+1}^-) - e^{-\nu H} z_2(t_{k+1}^-) \\ &= \int_{t_k}^{t_{k+1}} e^{(t_k-\ell)F_{22}} F_{21} w(\ell)\mathrm{d}\ell - \int_{t_k}^{t_{k+1}} e^{(t_k-\ell)H} G w(\ell)\mathrm{d}\ell \\ &+ \int_{t_k}^{t_{k+1}} e^{(t_k-\ell)F_{22}} f_2(w(\ell), u(\ell))\mathrm{d}\ell \\ &- \int_{t_k}^{t_{k+1}} e^{(t_k-\ell)H} f_3(w(\ell), u(\ell))\mathrm{d}\ell \end{aligned} \tag{49}$$

for all $k \geq 1$. By combining (45) with (48)-(49), we get

$$\begin{aligned} &Ex_r(t_{k+1}) - e^{-\nu H} Lr(t_{k+1}) \\ &= -Lr(t_k) + e^{-\nu F_{22}} z_1(t_{k+1}^-) - e^{-\nu H} z_2(t_{k+1}^-) \\ &+ \int_{t_k}^{t_{k+1}} \Lambda(t_k, \ell)(w(\ell) - r(\ell))\mathrm{d}\ell \\ &+ \int_{t_k}^{t_{k+1}} e^{(t_k-\ell)F_{22}}[f_2(r(\ell), u(\ell)) - f_2(w(\ell), u(\ell))]\mathrm{d}\ell \\ &- \int_{t_k}^{t_{k+1}} e^{(t_k-\ell)H}[f_3(r(\ell), u(\ell)) - f_3(w(\ell), u(\ell))]\mathrm{d}\ell \end{aligned} \tag{50}$$

where E was defined in (7) and

$$\Lambda(m, \ell) = e^{(m-\ell)H} G - e^{(m-\ell)F_{22}} F_{21}. \tag{51}$$

Therefore, since (36) gives

$$r(t_{k+1}) = r(s_{g(k+1)}) = y(s_{g(k+1)}) - \epsilon(s_{g(k+1)}), \tag{52}$$

it follows that

$$\begin{aligned} Ex_r(t_{k+1}) &= e^{-\nu H} Lr(t_{k+1}) - Lr(t_k) \\ &\quad + e^{-\nu F_{22}} z_1(t_{k+1}^-) - e^{-\nu H} z_2(t_{k+1}^-) \\ &\quad + \int_{t_k}^{t_{k+1}} \Lambda(t_k, \ell)(w(\ell) - r(\ell))\mathrm{d}\ell \\ &\quad + \int_{t_k}^{t_{k+1}} e^{(t_k-\ell)F_{22}} \Delta_2(\ell)\mathrm{d}\ell \\ &\quad - \int_{t_k}^{t_{k+1}} e^{(t_k-\ell)H} \Delta_3(\ell)\mathrm{d}\ell \end{aligned} \tag{53}$$

and so also

$$\begin{aligned} &Ex_r(t_{k+1}) = e^{-\nu H} Ly(t_{k+1}) - Ly(t_k) + L\epsilon(t_k) \\ &+ e^{-\nu F_{22}} z_1(t_{k+1}^-) - e^{-\nu H} z_2(t_{k+1}^-) - e^{-\nu H} L\epsilon(t_{k+1}) \\ &+ \int_{t_k}^{t_{k+1}} e^{(t_k-\ell)F_{22}} \Delta_2(\ell)\mathrm{d}\ell - \int_{t_k}^{t_{k+1}} e^{(t_k-\ell)H} \Delta_3(\ell)\mathrm{d}\ell \\ &+ \int_{t_k}^{t_{k+1}} \Lambda(t_k, \ell)(w(\ell) - r(\ell))\mathrm{d}\ell, \; k \geq 1 \end{aligned} \tag{54}$$

where

$$\Delta_i(\ell) = f_i(r(\ell), u(\ell)) - f_i(w(\ell), u(\ell)) \text{ for } i = 1, 2, 3. \tag{55}$$

Left multiplying (54) by E^{-1} and using the fact that

$$\begin{aligned} &R_1 z_1(t_{k+1}^-) + R_2 z_2(t_{k+1}^-) \\ &= z_1(t_{k+1}) + R_2 Ly(t_{k+1}) + E^{-1} Ly(t_k) \end{aligned} \tag{56}$$

which follows from (37), we conclude that

$$\begin{aligned} x_r(t_{k+1}) &= z_1(t_{k+1}) + E^{-1} L\epsilon(t_k) + R_2 L\epsilon(t_{k+1}) \\ &\quad + E^{-1} \int_{t_k}^{t_{k+1}} \Lambda(t_k, \ell)(w(\ell) - r(\ell))\mathrm{d}\ell \\ &\quad + E^{-1} \int_{t_k}^{t_{k+1}} e^{(t_k-\ell)F_{22}} \Delta_2(\ell)\mathrm{d}\ell \\ &\quad - E^{-1} \int_{t_k}^{t_{k+1}} e^{(t_k-\ell)H} \Delta_3(\ell)\mathrm{d}\ell, \text{ if } k \geq 1. \end{aligned} \tag{57}$$

Second part of the proof: upper bounding $w(t) - r(t)$. We next use the variables

$$\tilde{w}(t) = w(t) - r(t) \text{ and } \tilde{x}_r(t) = x_r(t) - z_1(t). \tag{58}$$

Then it follows from (3) and (37) that

$$\begin{aligned} \dot{\tilde{w}}(t) &= F_{11}\tilde{w}(t) - F_{12}\tilde{x}_r(t) + f_1(w(t), u(t)) \\ &\quad - f_1(r(t), u(t)) \text{ if } t \in [s_k, s_{k+1}) \\ \tilde{w}(s_k) &= \epsilon(s_k) \end{aligned} \tag{59}$$

for all $k \in \mathbb{N}$. By applying variation of parameters to the first equation in (59) on any interval $[s_k, t]$, we then get

$$\begin{aligned} \tilde{w}(t) &= e^{F_{11}(t-s_k)}\epsilon(s_k) \\ &\quad - \int_{s_k}^{t} e^{F_{11}(t-m)} \left[\Delta_1(m) + F_{12}\tilde{x}_r(m)\right] \mathrm{d}m \end{aligned} \tag{60}$$

if $t \in [s_k, s_{k+1})$ and $k \in \mathbb{N}$. By (13) and (60), it follows that

$$\begin{aligned} |\tilde{w}(t)| &\leq \mathcal{F}_\mu(F_{11})|\epsilon(s_k)| + \mathcal{I}_+^\mu(F_{11})\big(f_{\dagger,1}|\tilde{w}|_{[t-\mu,t]} \\ &\quad + |F_{12}||\tilde{x}_r|_{[t-\mu,t]}\big) \text{ if } t \in [s_k, s_{k+1}) \end{aligned} \tag{61}$$

for all $k \in \mathbb{N}$, by the definition of the sequence s_k.

Third part of the proof: an upper bound for $\tilde{x}_r(t)$.

By combining (57) with (3) and (37), we obtain

$$\begin{aligned}\dot{\tilde{x}}_r(t) &= F_{22}\tilde{x}_r(t) - F_{21}\tilde{w}(t)\\ &\quad +\Delta_2(t) \text{ if } t \in [t_k, t_{k+1})\\ \tilde{x}_r(t_{k+1}) &= E^{-1}\int_{t_k}^{t_{k+1}} \Lambda(t_k,\ell)\tilde{w}(\ell)\mathrm{d}\ell\\ &\quad +E^{-1}\int_{t_k}^{t_{k+1}} e^{(t_k-\ell)F_{22}}\Delta_2(\ell)\mathrm{d}\ell\\ &\quad -E^{-1}\int_{t_k}^{t_{k+1}} e^{(t_k-\ell)H}\Delta_3(\ell)\mathrm{d}\ell\\ &\quad +R_2L\epsilon(t_{k+1}) + E^{-1}L\epsilon(t_k)\end{aligned} \tag{62}$$

for all integers $k \geq 1$. By applying variation of parameters to the first equation of (62) on any interval $[t_k, t]$ with $t \in [t_k, t_{k+1})$, it follows from our formula for Δ_2 from (55) and our condition (14) on $f_{\dagger,2}$ that we have

$$\begin{aligned}|\tilde{x}_r(t)| &\leq \mathcal{F}_\nu(F_{22})|\tilde{x}_r(t_k)|\\ &\quad + \int_{t_k}^{t} \left|e^{F_{22}(t-\ell)}\right|\left[|F_{21}||\tilde{w}(\ell)| + f_{\dagger,2}|\tilde{w}(\ell)|\right]\mathrm{d}\ell\\ &\leq \mathcal{F}_\nu(F_{22})|\tilde{x}_r(t_k)|\\ &\quad +\mathcal{I}_+^\nu(F_{22})\big(|F_{21}| + f_{\dagger,2}\big)|\tilde{w}|_{[t-\nu,t]},\ k \geq 1.\end{aligned} \tag{63}$$

On the other hand, using the second equality in (62) to upper bound the $|\tilde{x}_r(t_k)|$ term in (63) gives

$$\begin{aligned}|\tilde{x}_r(t)| &\leq \mathcal{F}_\nu(F_{22})\overline{E}\int_{t_{k-1}}^{t_k} |\Lambda(t_{k-1},\ell)||\tilde{w}(\ell)|\mathrm{d}\ell\\ &\quad +\mathcal{F}_\nu(F_{22})\overline{E}\mathcal{I}_-^\nu(F_{22})f_{\dagger,2}|\tilde{w}|_{[t-2\nu,t]}\\ &\quad +\mathcal{F}_\nu(F_{22})\overline{E}\mathcal{I}_-^\nu(H)f_{\dagger,3}|\tilde{w}|_{[t-2\nu,t]}\\ &\quad +\mathcal{F}_\nu(F_{22})(|R_2L| + |E^{-1}L|)|\epsilon|_{[t-2\nu,t]}\\ &\quad +\mathcal{I}_+^\nu(F_{22})\big(|F_{21}| + f_{\dagger,2}\big)|\tilde{w}|_{[t-\nu,t]}\end{aligned} \tag{64}$$

for all $k \geq 2$ and $t \in [t_k, t_{k+1})$ with $f_{\dagger,3}$ as defined in (16) and $\bar{E}$ defined in (15). Then our formula (51) for Λ gives

$$\begin{aligned}&|\tilde{x}_r(t)| \leq \mathcal{F}_\nu(F_{22})(|R_2L| + |E^{-1}L|)|\epsilon|_{[t-2\nu,t]}\\ &+ \mathcal{F}_\nu(F_{22})\overline{E}\left(\mathcal{I}_-^\nu(H)|G| + \mathcal{I}_-^\nu(F_{22})|F_{21}|\right)|\tilde{w}|_{[t_{k-1},t_k]}\\ &+\overline{E}\mathcal{F}_\nu(F_{22})(\mathcal{I}_-^\nu(F_{22})f_{\dagger,2} + \mathcal{I}_-^\nu(H)f_{\dagger,3})|\tilde{w}|_{[t-2\nu,t]}\\ &+\mathcal{I}_+^\nu(F_{22})(|F_{21}| + f_{\dagger,2})|\tilde{w}|_{[t-\nu,t]}.\end{aligned} \tag{65}$$

Hence, our choice of β from (40) gives

$$\begin{aligned}|\tilde{x}_r(t)| &\leq \beta(\nu)|\tilde{w}|_{[t-2\nu,t]}\\ &\quad +\mathcal{F}_\nu(F_{22})(|R_2L|+|E^{-1}L|)|\epsilon|_{[t-2\nu,t]}\end{aligned} \tag{66}$$

for all $t \in [t_k, t_{k+1})$ and $k \geq 2$.

Fourth part of the proof: stability and robustness analysis.

Grouping (61) and (66), and recalling that $s_{k+1} - s_k = \mu$ for all $k \in \mathbb{Z}_{\geq 0}$, we obtain

$$\begin{aligned}|\tilde{x}_r(t)| &\leq \beta(\nu)|\tilde{w}|_{[t-2\nu,t]} + \mathcal{M}_\nu|\epsilon|_{[t-2\nu,t]}\\ |\tilde{w}(t)| &\leq \mathcal{I}_+^\mu(F_{11})\big(f_{\dagger,1}|\tilde{w}|_{[t-\mu,t]} + |F_{12}||\tilde{x}_r|_{[t-\mu,t]}\big)\\ &\quad +\mathcal{F}_\mu(F_{11})|\epsilon|_{[t-\mu,t]}\end{aligned} \tag{67}$$

for all $t \geq 2\nu$, where $\mathcal{M}_\nu = \mathcal{F}_\nu(F_{22})(|R_2L| + |E^{-1}L|)$. Combining the inequalities in (67), we obtain

$$\begin{aligned}|\tilde{x}_r(t)| &\leq \beta(\nu)\mathcal{I}_+^\mu(F_{11})f_{\dagger,1}|\tilde{w}|_{[t-\mu-2\nu,t]}\\ &\quad + \beta(\nu)\mathcal{I}_+^\mu(F_{11})|F_{12}||\tilde{x}_r|_{[t-\mu-2\nu,t]}\\ &\quad + \left[\mathcal{M}_\nu + \beta(\nu)\mathcal{F}_\mu(F_{11})\right]|\epsilon|_{[t-(2\nu+\mu),t]}\\ |\tilde{w}(t)| &\leq \mathcal{I}_+^\mu(F_{11})f_{\dagger,1}|\tilde{w}|_{[t-\mu,t]} + \mathcal{F}_\mu(F_{11})|\epsilon|_{[t-\mu,t]}\\ &\quad +\mathcal{I}_+^\mu(F_{11})|F_{12}||\tilde{x}_r|_{[t-\mu,t]}\end{aligned} \tag{68}$$

for all $t \geq 4\nu$. Setting $\varsigma(t) = |\tilde{x}_r(t)| + |\tilde{w}(t)|$, it follows from the inequalities in (68) that

$$\begin{aligned}&\varsigma(t) \leq \mathcal{I}_+^\mu(F_{11})\big(\beta(\nu)+1\big)\max\{f_{\dagger,1}, |F_{12}|\}|\varsigma|_{[t-\mu-2\nu,t]}\\ &+\big(\mathcal{M}_\nu + \mathcal{F}_\mu(F_{11})(\beta(\nu) + 1)\big)|\epsilon|_{[t-\mu-2\nu,t]}\end{aligned} \tag{69}$$

for all $t \geq 4\nu$. Setting $\mathcal{M}_a = \mathcal{M}_\nu + \mathcal{F}_\mu(F_{11})(\beta(\nu)+1)$, and recalling our choice (40) of γ and the fact that $\gamma(\mu) \in (0,1)$, it now follows from applying (Mazenc *et al.*, 2017, Lemma 1) to the function $X(t) = \varsigma(t + m)$ that

$$\varsigma(t) \leq e^{\frac{\ln(\gamma(\mu))}{\mu+2\nu+m}(t-m)}|\varsigma|_{[m-(\mu+2\nu),m]} + \frac{\mathcal{M}_a|\epsilon|_{[t-2\nu-\mu,t]}}{1-\gamma(\mu)} \tag{70}$$

if $t \geq m \geq 4\nu$. We conclude that

$$\begin{aligned}&|\tilde{x}_r(t)| \leq \frac{\mathcal{M}_a}{1-\gamma(\mu)}|\epsilon|_{[t-2\nu-\mu,t]}\\ &+e^{\frac{\ln(\gamma(\mu))}{\mu+2\nu+m}(t-m)}\left(|\tilde{x}_r|_{[m-(\mu+2\nu),m]} + |\tilde{w}|_{[m-(\mu+2\nu),m]}\right)\end{aligned} \tag{71}$$

if $t \geq m \geq 4\nu$. The result now follows from our choice of $\mathcal{M}_*$ from (42) and our choices (58) of $\tilde{x}_r$ and $\tilde{w}$.

5 Illustrations

We next provide two illustrations of Theorems 1-2. Our first illustration uses the robotic manipulator dynamic from Zhao and Jiang (2019), and improves on Zhao and Jiang (2019) by using a new change of variables that leads to a reduced-order fixed time converging observer that converges for all initial states. Our second illustration uses a pendulum dynamics. In each case, we obtain a globally Lipschitz f, so we are able to apply both theorems to obtain the enhanced ISS properties with respect to measurement error.

5.1 Robotic Manipulator

Consider a single-link robotic manipulator coupled to a DC motor with a nonrigid joint. As noted in (Krstic *et al.*, 1995, Section 7.3.3, p.313) and Zhao and Jiang (2019), if we model the joint as a linear torsional spring, the dynamics can be modeled by

$$\left\{\begin{aligned}J_1\ddot{q}_1(t) &= -F_1\dot{q}_1(t) - K\left(q_1(t) - \frac{q_2(t)}{N}\right)\\ &\qquad - mg_*d\cos(q_1(t))\\ J_2\ddot{q}_2(t) &= -F_2\dot{q}_2(t) + \frac{K}{N}\left(q_1(t) - \frac{q_2(t)}{N}\right) + K_t\mathcal{I}(t)\\ \mathcal{L}\dot{\mathcal{I}}(t) &= -R\mathcal{I}(t) - K_b\dot{q}_2(t) + u_*(t),\end{aligned}\right. \tag{72}$$

where q_1 and q_2 are the angular positions of the link and the motor shaft respectively, $\mathcal{I}$ and u_* are the armature current and voltage respectively, the positive constants J_1 and J_2

are the inertias, the positive constants F_1 and F_2 are the viscous friction constants, K is the positive spring constant, K_t is the positive torque constant, K_b is the positive back EMF constant, R and $\mathcal{L}$ are the armature resistance and inductance respectively and are positive constants, m is the constant positive link mass, the positive constant d is the position of the link's center of gravity, $N > 0$ is the positive gear ratio, and $g_* > 0$ is the constant gravity acceleration.

The works Krstic *et al.* (1995) and Zhao and Jiang (2019) provided asymptotic convergence results and finite time observers for (72) with a convergence time that depends on the initial state, and both works assumed that the only state available for measurement was q_1. This left open the important question of whether one can achieve fixed time convergence of observers, i.e., a convergence time for observers for (72) that is independent of the initial state, with corresponding ISS properties under measurement error as in our theorems above. In this subsection, we show that such a fixed time converging observer can be constructed using our Theorem 1 when one has measurements of q_1.

To this end, observe that in terms of the new variables

$$\begin{aligned} & x_1(t) = q_1(t),\ x_2(t) = \dot{q}_1(t), \\ & x_3(t) = \tfrac{K}{J_1 N} q_2(t) - \tfrac{m g_* d}{J_1},\ \ x_4(t) = \tfrac{K}{J_1 N}\dot{q}_2(t) \\ & x_5(t) = \tfrac{K K_t}{J_1 J_2 N}\mathcal{I}(t) - \tfrac{K m g_* d}{J_1 J_2 N^2} \\ & \text{and}\ \ u(t) = u_*(t) - \tfrac{m g_* d R}{K_t N}, \end{aligned} \tag{73}$$

we obtain the new system

$$\begin{cases} \dot{x}_1(t) = x_2(t) \\ \dot{x}_2(t) = -\tfrac{F_1}{J_1}x_2(t) - \tfrac{K}{J_1}x_1(t) + x_3(t) \\ \qquad\quad + \tfrac{m g_* d}{J_1}[1-\cos(x_1(t))] \\ \dot{x}_3(t) = x_4(t) \\ \dot{x}_4(t) = \tfrac{K^2}{N^2 J_1 J_2}x_1(t) - \tfrac{K}{N^2 J_2}x_3(t) \\ \qquad\quad - \tfrac{F_2}{J_2}x_4(t) + x_5(t) \\ \dot{x}_5(t) = -\tfrac{R}{\mathcal{L}}x_5(t) - \tfrac{K_t K_b}{J_2 \mathcal{L}}x_4(t) + \tfrac{K K_t}{J_1 J_2 N \mathcal{L}}u(t). \end{cases} \tag{74}$$

The system (74) has the form (1) with $n = 5$, $p = 1$, and

$$A = \begin{bmatrix} 0 & 1 & 0 & 0 & 0 \\ -\frac{K}{J_1} & -\frac{F_1}{J_1} & 1 & 0 & 0 \\ 0 & 0 & 0 & 1 & 0 \\ \frac{K^2}{N^2 J_1 J_2} & 0 & -\frac{K}{N^2 J_2} & -\frac{F_2}{J_2} & 1 \\ 0 & 0 & 0 & -\frac{K_b K_t}{J_2 \mathcal{L}} & -\frac{R}{\mathcal{L}} \end{bmatrix},$$

$$f(r,u) = \begin{bmatrix} 0 \\ \frac{m g_* d}{J_1}[1-\cos(x_1)] \\ 0 \\ 0 \\ \frac{K_t K}{J_1 J_2 N \mathcal{L}}u \end{bmatrix}, \tag{75}$$

$$\text{and } C = \begin{bmatrix} 1 & 0 & 0 & 0 & 0 \end{bmatrix},$$

where $r = Cx$. Then C has full rank. Choosing

$$\mho = [V^\top\ C^\top]^\top,\ \text{where } V = [0_{4\times 1}\ I_4], \tag{76}$$

we obtain

$$\mho A \mho^{-1} = \begin{bmatrix} F_{22} & F_{21} \\ F_{12} & F_{11} \end{bmatrix},\ f_1 = Cf,\ \text{and } f_2 = Vf. \tag{77}$$

Therefore, the coefficient matrices and the functions f_i for $i = 1$ and 2 in (3) are

$$F_{11} = 0,\ \ F_{12} = \begin{bmatrix} 1 & 0 & 0 & 0 \end{bmatrix},\ f_1(r,u) = 0,$$

$$F_{22} = \begin{bmatrix} -\frac{F_1}{J_1} & 1 & 0 & 0 \\ 0 & 0 & 1 & 0 \\ 0 & -\frac{K}{N^2 J_2} & -\frac{F_2}{J_2} & 1 \\ 0 & 0 & -\frac{K_b K_t}{J_2 \mathcal{L}} & -\frac{R}{\mathcal{L}} \end{bmatrix},$$

$$f_2(r,u) = \begin{bmatrix} \frac{m g_* d}{J_1}[1-\cos(x_1)] \\ 0 \\ 0 \\ \frac{K_t K u}{J_1 J_2 N \mathcal{L}} \end{bmatrix},\ \text{and } F_{21} = \begin{bmatrix} -\frac{K}{J_1} \\ 0 \\ \frac{K^2}{N^2 J_1 J_2} \\ 0 \end{bmatrix}.$$

Following Zhao and Jiang (2019), we now specialize to the case where $F_1 = F_2 = J_1 = J_2 = K = N = R = \mathcal{L} = K_b = K_t = 1$, $m = 1/2$, $g_* = 10$, and $d = 1/5$. Then (A, C) is observable, and simple MATLAB calculations show that our requirements from Section 2 are satisfied with $\nu = 2$ and

$$L = [1\ \ 0\ \ 1\ \ 0]^\top, \tag{78}$$

so Theorem 1 applies.

To illustrate the efficacy of Theorem 1, we provide MATLAB simulations in Figures 1-2 that show tracking error components that we obtained when we applied our observer design to the preceding robotic manipulator dynamics with the preceding parameter values. Figure 2 is used to show the effects of the perturbation term ϵ in the output. We used the control

$$\begin{aligned} u(t) = -\lambda\Big(& [\lambda^4 y(t)]^{5\kappa-4} + 5[\lambda^3 z_{11}(t)]^{\frac{5\kappa-4}{\kappa}} \\ & + 10[\lambda^2 z_{12}(t)]^{\frac{5\kappa-4}{2\kappa-1}} \\ & + 10[\lambda z_{13}(t)]^{\frac{5\kappa-4}{3\kappa-2}} + 5[z_{14}(t)]^{\frac{5\kappa-4}{4\kappa-3}}\Big) \end{aligned} \tag{79}$$

from Zhao and Jiang (2019), with the choices $\lambda = 3$ and $\kappa = 1$, where z_{1k} denotes the ith element of the vector z_1 for $k = 1, 2, 3, 4$. We used

$$\epsilon(t) = 0.03 \sum_{w=1}^{50} \sin(wt) \tag{80}$$

in our simulation with measurement error. We also set $\tilde{x}_{rk} = x_{rk} - z_{1k}$, where x_{rk} is the kth component of x_r, for each k. Since Figures 1-2 indicate finite time convergence at time $t_2 = 2\nu = 4$ when $\epsilon = 0$ and our robustness property from Theorem 1 when (80) is the measurement error, they help illustrate Theorem 1 in the special case of the

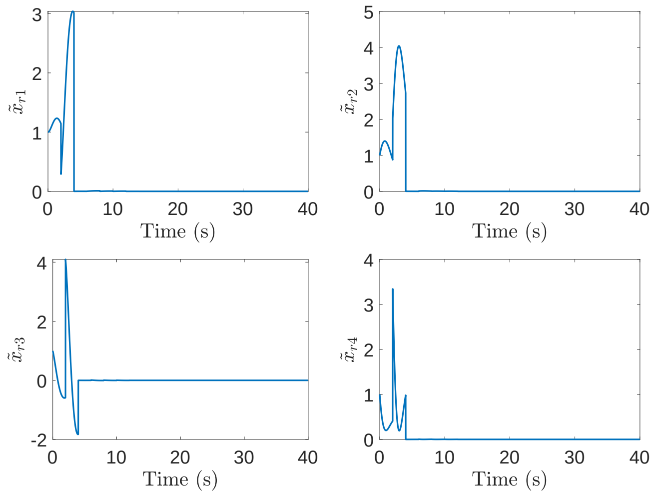

Fig. 1. Simulation for (74) using Theorem 1 and $\epsilon = 0$ and fixed convergence time 4

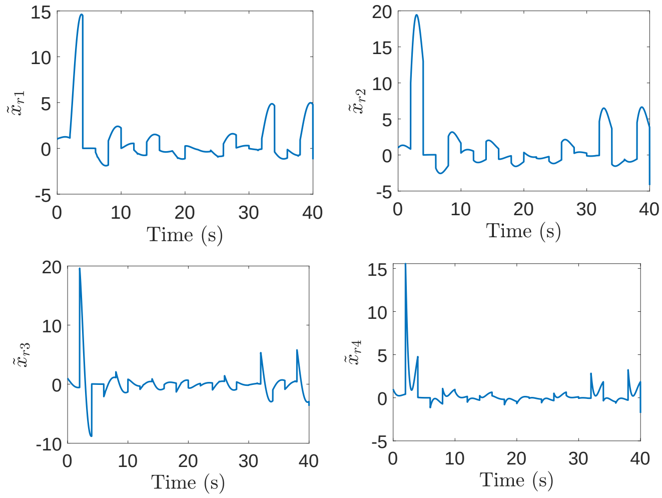

Fig. 2. Simulation for (74) using Theorem 1 and (80) robotic manipulator dynamics.

5.2 *Pendulum*

In this section, we illustrate Theorem 2. As in Dinh *et al.* (2015), we study a pendulum model

$$\begin{cases} \dot{x}_1(t) &= x_2(t) \\ \dot{x}_2(t) &= -\sin(x_1(t)), \\ y(t) &= x_1(s_j) + \epsilon(s_j) \ \text{ if } t \in [s_j, s_{j+1}) \end{cases} \tag{81}$$

with $x_1(t)$ and $x_2(t)$ both valued in $\mathbb{R}$.

With the notation of the previous sections, we have

$$\begin{cases} \dot{r}(t) &= x_r(t) \\ \dot{x}_r(t) &= f_2(r(t), u(t)) \\ y(t) &= r(s_j) + \epsilon(s_j) \ \text{ if } t \in [s_j, s_{j+1}) \end{cases} \tag{82}$$

with $f_1(r, u) = 0$ and $f_2(r, u) = -\sin(r)$. This produces the coefficient matrices

$$F_{11} = F_{22} = F_{21} = 0 \text{ and } F_{12} = 1. \tag{83}$$

We can choose $L = -1$ and any constant $\nu > 0$. This provides the values

$$\begin{aligned} &H = -1, \ G = -1, \ E = 1 - e^{\nu}, \\ &R_1 = \tfrac{1}{1-e^{\nu}}, \ R_2 = -\tfrac{e^{\nu}}{1-e^{\nu}}, \text{ and } f_3 = f_2. \end{aligned} \tag{84}$$

Assumptions 1-3 are satisfied with

$$A = \begin{bmatrix} 0 & 1 \\ 0 & 0 \end{bmatrix} \text{ and } C = [1 \quad 0]. \tag{85}$$

Then Theorem 2 applies. It yields the observer

$$\begin{cases} \dot{z}_1(t) &= -\sin(w(t), \text{ if } t \in [s_{gk}, s_{g(k+1)}) \\ \dot{z}_2(t) &= -z_2(t) - w(t) - \sin(w(t) \\ & \quad \text{if } t \in [s_{gk}, s_{g(k+1)}) \\ z_1(s_{g(k+1)}) &= \tfrac{1}{1-e^{\nu}} z_1(s^-_{g(k+1)}) - \tfrac{e^{\nu}}{1-e^{\nu}} z_2(s^-_{g(k+1)}) \\ & \quad -\tfrac{e^{\nu}}{1-e^{\nu}} y(s_{g(k+1)}) + \tfrac{1}{1-e^{\nu}} y(s_{gk}) \\ z_2(s_{g(k+1)}) &= \tfrac{1}{1-e^{\nu}} z_1(s^-_{g(k+1)}) - \tfrac{e^{\nu}}{1-e^{\nu}} z_2(s^-_{g(k+1)}) \\ & \quad -\tfrac{e^{\nu}}{1-e^{\nu}} y(s_{g(k+1)}) + \tfrac{1}{1-e^{\nu}} y(s_{gk}) \\ \dot{w}(t) &= z_1(t) \text{ if } t \in [s_k, s_{k+1}) \\ w(s_k) &= y(s_k) \end{cases} \tag{86}$$

with $z_1(0) = z_2(0) = 0$, where $s_i = i\mu$ for all integers $i \geq 0$, and where $\mu = \nu/g$. For any constant $\epsilon_0 > 0$, we choose

$$f_{\dagger,1} = \epsilon_0 \text{ and } f_{\dagger,2} = 1 \tag{87}$$

to obtain $f_{\dagger,3} = 1 + \epsilon_0$ and so also

$$\begin{aligned} &\beta(\nu) = \tfrac{(\nu+2+\epsilon_0)e^{\nu}-2-\epsilon_0}{e^{\nu}-1} \\ &\text{and } \ \gamma(\mu) = \mu\left(\tfrac{(\nu+2+\epsilon_0)e^{\nu}-2-\epsilon_0}{e^{\nu}-1} + 1\right)\epsilon_0. \end{aligned} \tag{88}$$

If we now choose $\nu = 1$, then our requirement $\gamma(\mu) < 1$ from Theorem 2 is satisfied for any $g \geq 5$ and $\mu = 1/g$ for a small enough $\epsilon_0 > 0$, and a lower bound for the convergence rate of our observer from Theorem 2 is given by

$$-\frac{\ln(\gamma(\mu))}{\mu + 2 + 1}, \tag{89}$$

where we took $m = \nu = 1$, and (89) converges to $+\infty$ as $\mu \to 0^+$, or equivalently, as $g = 1/\mu \to +\infty$ with $g \in \mathbb{N}$.

In Figures 3-4 below, we provide results from our MATLAB simulations that used the observer design from Theorem 2 and the preceding pendulum dynamics with the preceding parameter choices and $\nu = 1$ and $g = 6$, where we again used the choice (80) of the measurement error in the perturbed case. Figure 4 shows the effects of the perturbation term ϵ in the output measurement.

We use the notation $\tilde{x}_r = x_r - z_1$. Since the simulations exhibit rapid convergence of the observation error to zero without measurement error, and the required robustness property under measurement error, they illustrate the efficacy of Theorem 2 in the special case of the pendulum dynamics.

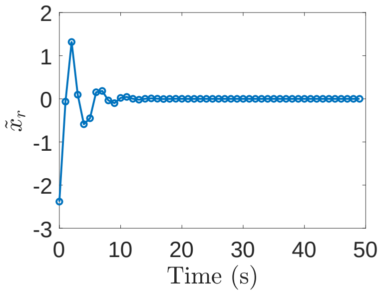

Fig. 3. Simulation of (81) with measurement error $\epsilon = 0$

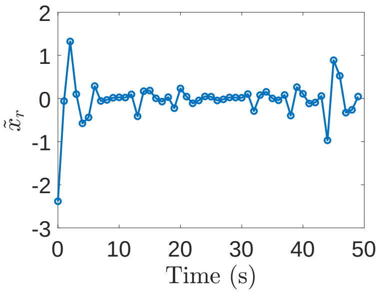

Fig. 4. Simulation of (81) with measurement error (80)

6 Conclusions

We advanced control theory for reduced-order observers, using a method to achieve arbitrarily fast convergence of the observation error to zero. We provided two families of continuous-discrete reduced-order observers for systems with continuous or discrete measurements and measurement error. When continuous observations are available, the reduced-order observer has dimension $2(n-p)$ where n (resp., p) is the dimension of the original system (resp., the output) and enjoys fixed time convergence, i.e., finite time convergence with a convergence time that is independent of the initial state. When only discrete measurements are available, our observer has dimension $2n - p$, and a convergence rate that can be made arbitrarily large. In both cases, our observers enjoy a robustness property in which the overshoot term in the ISS type estimate only depends on a recent history of the measurement error.

References

Ahmed, S., F. Mazenc and H. Ozbay (2018). Dynamic output feedback stabilization of switched linear systems with delay via a trajectory based approach. *Automatica* **93**, 92–97.

Ahmed, S., M. Malisoff and F. Mazenc (2019). Finite time estimation for time-varying systems with delay in the measurements. *Systems and Control Letters* **133**, 104551.

Besançon, G. (2007). *Nonlinear Observers and Applications*. Springer Verlag. New York, NY.

Dinh, T., V. Andrieu, M. Nadri and U. Serres (2015). Continuous-discrete time observer design for Lipschitz systems with sampled measurements. *IEEE Transactions on Automatic Control* **60**(3), 787–792.

Engel, R. and G. Kreisselmeier (2002). A continuous time observer which converges in finite time. *IEEE Transactions on Automatic Control* **47**(7), 1202–1204.

Karafyllis, I. and C. Kravaris (2009). From continuous-time design to sampled-data design of observers. *IEEE Transactions on Automatic Control* **54**(9), 2169–2174.

Karafyllis, I. and Z.P. Jiang (2013). Reduced-order dead-beat observers for the chemostat. *Nonlinear Analysis Series B: Real World Applications* **14**(1), 340–351.

Krstic, M., I. Kanellakopoulos and P. Kokotovic (1995). *Nonlinear and Adaptive Control Design*. Wiley Interscience. New York, NY.

Lebastard, V., Y. Aoustin and F. Plestan (2006). Observer-based control of a walking biped robot without orientation measurement. *Robotica* **24**(3), 385–400.

Lopez-Ramirez, F., A. Polyakov, D. Efimov and W. Perruquetti (2018). Finite-time and fixed-time observer design: Implicit Lyapunov function approach. *Automatica* **87**, 52–60.

Luenberger, D. (1979). *Introduction to Dynamic Systems*. John Wiley and Sons. New York.

Mazenc, F., E. Fridman and W. Djema (2015). Estimation of solutions of observable nonlinear systems with disturbances. *Systems and Control Letters* **79**, 47–58.

Mazenc, F., M. Malisoff and S-I. Niculescu (2017). Stability and control design for time-varying systems with time-varying delays using a trajectory-based approach. *SIAM Journal on Control and Optimization* **55**(1), 533–556.

Mazenc, F., M. Malisoff and Z.P. Jiang (2020). Reduced order fast converging observer for systems with discrete measurements. In Proceedings of the 24th International Symposium on Mathematical Theory of Networks and Systems. Cambridge, UK.

Menard, T., E. Moulay and W. Perruquetti (2010). A global high-gain finite time observer. *IEEE Transactions on Automatic Control* **55**(6), 1500–1506.

Menard, T., E. Moulay and W. Perruquetti (2017). Fixed-time observer with simple gains for uncertain systems. *Automatica* **81**, 438–446.

Raff, T. and F. Allgower (2008). An observer that converges in finite time due to measurement-based state updates. *IFAC Proceedings Volumes* **41**(2), 2693–2695.

Raff, T., P. Menold, C. Ebenbauer and F. Allgower (2005). Finite time functional observer for linear systems. In Proceedings of the IEEE Conference on Decision and Control. Seville, Spain. pp. 7198–7203.

Sanchez-Torres, J., A. Loukianov, J. Moreno and S. Drakunov (2012). An equivalent control based sliding mode observer using high order uniform robust sliding operators. In Proceedings of the American Control Conference. Montreal, Canada. pp. 6160–6165.

Sauvage, F., M. Guay and D. Dochain (2007). Design of a nonlinear finite time converging observer for a class of nonlinear systems. *Journal of Control Science and Engineering* **2007**(36954), 9pp.

Zhao, Z.-L. and Z.P. Jiang (2019). Semi-global finite-time output-feedback stabilization with an application to robotics. *IEEE Transactions on Industrial Electronics* **66**(4), 3148–3156.